SUPPLEMENT

Effect of intranasal oxytocin on resting-state effective connectivity in schizophrenia

Vittal Korann[+1], Arpitha Jacob[+1], Bonian Lu[2], Priyanka Devi[1], Umesh Thonse [1], Bhargavi Nagendra[1], Dona Maria Chacko[1], Avyarthana Dey[1], Anantha Padmanabha[1], Venkataram Shivakumar, Rose Dawn Bharath[1], Vijay Kumar[1], Shivarama Varambally[1], Ganesan Venkatasubramanian[1], Gopikrishna Deshpande[2,3,4#], Naren P Rao[1#*]

[1 -] National Institute of Mental Health and Neurosciences, Bangalore, Karnataka, India
[2-] AU MRI Research Center, Department of Electrical and Computer Engineering, Auburn University, Auburn, Alabama, USA
[3-] Department of Psychological Sciences, Auburn University, Auburn, Alabama, USA
[4-] Center for Neuroscience, Auburn University, Auburn, Alabama, USA

Oxytocin preparation and administration:

A commercially available oxytocin was purchased for the study (Victoria pharmaceuticals, Zurich, Switzerland). A single investigator handed the bottles to participants and supervised the administration. Oxytocin or 0.9% saline were prepared and placed in the bottle. The bottles were identical looking and were not labeled to preserve blinding. The investigator supervising (AJ) the administration was present with the subject during the administration. The participants were asked to be seated in the head upright position. Participants were asked to clean the nose before administration and all those with nasal congestion were excluded. After a test spray, the participants inserted the spray bottle tip into the nose and self-administered 3 puffs per nostril (4 IU of oxytocin/puff for a total dose of 24 IU). The puffs were alternated between nostrils so that an interval is given between puffs in the same nostril. The order of administration of oxytocin and placebo

Figure S1- overview of the study design

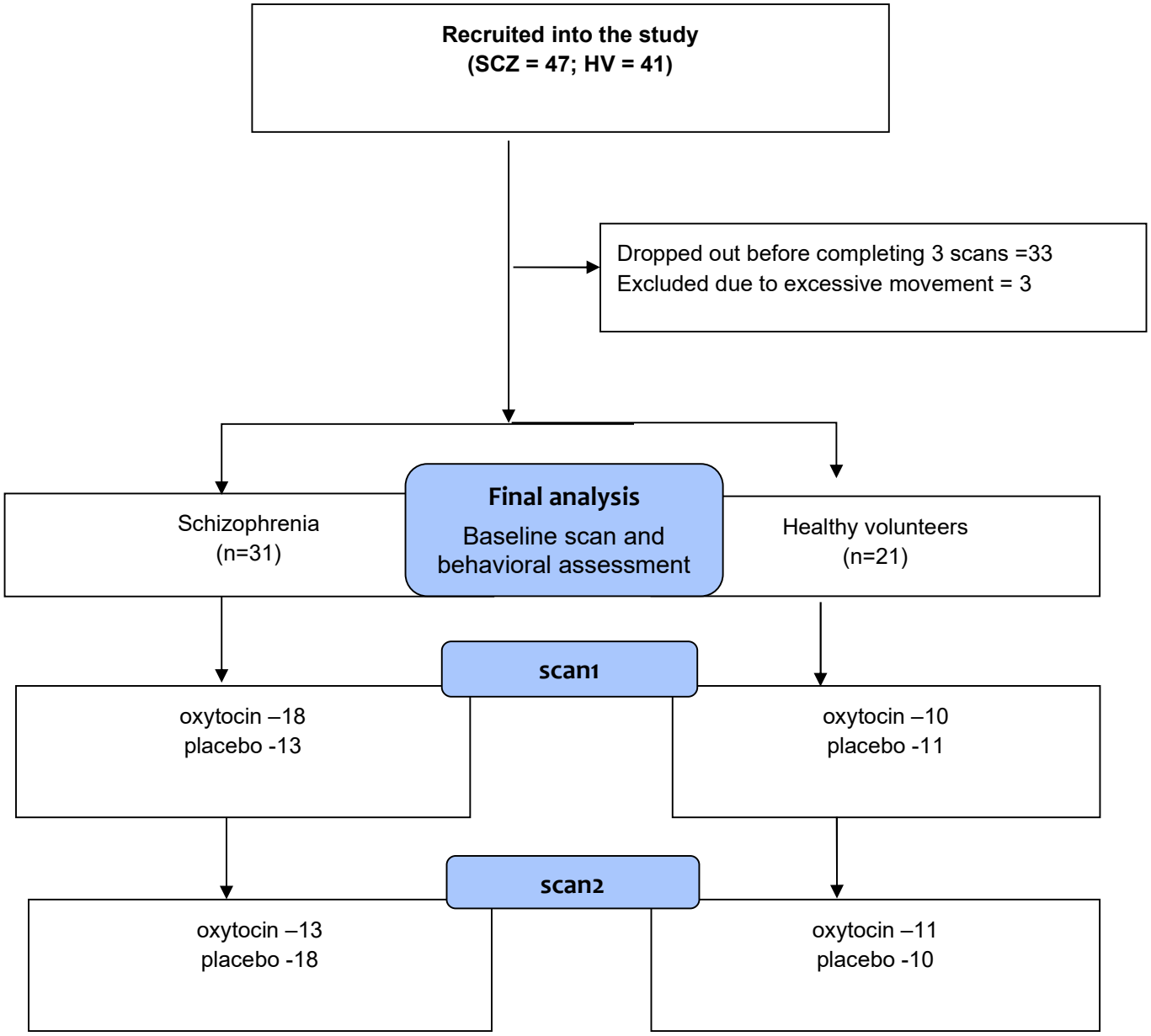

Description of Effective Connectivity Analysis:

Whole-brain effective connectivity (EC) was obtained using Granger causality. Granger causality is an exploratory technique used to quantify directional influences between brain regions. The underlying concept is that, if past values of a timeseries 'T1' can, in a mathematical sense, predict the future values of another timeseries 'T2' then a causal influence from timeseries T1 to timeseries T2 is inferred [Granger, 1969]. Granger causality employs a multivariate vector autoregressive (MVAR) model to quantitatively predict one timeseries using the other, which is briefly described next.

Given a system defined by k different timeseries $X(t) = [x_1(t), x_2(t), \ldots x_k(t)]$, with k being 90 ROIs in this study, the traditional MVAR model of order p is given by:

$$X(t) = A(1)X(t-1) + X(2)X(t-2) + \ldots A(p)X(t-p) + E(T) \qquad \text{-----(1)}$$

Where E(t) is the model error and A(1) ... A(p) are the model coefficients. The coefficients were estimated through multivariate least squares estimation, which calculates the optimal set of coefficients that minimizes the model error in the least squares sense. Model order p must be chosen either by employing a mathematical principle such as the Bayesian Information Criterion (BIC) [1] or based on the requirements of the application under consideration. In neuroimaging, the interest is in causal relationships within neural delays of a TR [2], thus we chose a first order model. Since fMRI's temporal resolution is low, a first order model is shown to capture the most relevant causal information [2].

Coefficient A(p) indicates the degree to which the past X(t-p) can predict the present X(t). Then, the sum of coefficients of all delays would represent the degree to which all the past values together can predict the present. This formulation is used to evaluate Granger causality by predicting the present value of timeseries-2 (T2) using the past values of timeseries-1 (T1). If, for example, the sum of the resulting model coefficients is large, then it implies that T1 can predict T2 very well. If T1's past can predict T2's present, then that implies a causal relationship from T1 to T2. As in previous studies [2], Granger causality (GC) was derived formally, based on the model coefficients, as:

$$GC_{ij} = \sum_{n=1}^{P} a_{ij}(n) \qquad \text{-----(2)}$$

Where GC_{ij} is the EC value from ROI i to ROI j and a_{ij} are the elements of matrix A. It is notable that a single coefficient matrix is obtained for the entire duration of data, and the coefficients do not vary over time. This traditional formulation of Granger causality was slightly modified, as in earlier studies [3], to remove the effect of zero-lag cross correlation between timeseries. For this, we included the zero-lag term in Eq.1 as shown below.

$$X(t) = A'(0)X(t) + A'(1)X(t-1) + A'(2)X(t-2) + \ldots$$
$$+ A'(p)\, X(t-p) + E(t) \qquad \text{---- (3)}$$

The diagonal elements of A(0) are set to zero, such that only the instantaneous cross correlation, and not autocorrelation, between the timeseries are modeled. The model coefficients obtained from Eq.3 would not be equal to those obtained from Eq.1, since the inclusion of zero-lag term affects other coefficients by removing cross-correlation effects from them. The zero-lag term is thus not used in the evaluation of Granger causality. Granger causality thus obtained would be free from zero-lag correlation effects and is defined as correlation-purged Granger causality (CPGC), which has been widely used in recent times.

A Granger causality value of 0 represents no causal relationship from the source to the destination region, a value of 1 represents strong positive causality (increase in BOLD response of the source region causes an increase in BOLD response of the destination, and vice versa), and a value of -1 represents strong negative causality (increase in BOLD response of the source region causes decrease in BOLD response of the destination, and vice versa). Recent simulations [4, 5] as well as experimental results [6–8] suggest that GC applied after deconvolving the HRF from fMRI data (as we have done), is reliable for making inferences about directional influences between brain regions. In fact, in a rat model of epilepsy with concurrent neuroimaging and invasive electrophysiological data, Dynamic Causal Modeling (DCM) and Granger causality applied on deconvolved data were the only methods that reproduced the electrophysiological ground truth [9]. Since our study is exploratory, we have opted to use Granger causality instead of DCM, and future confirmatory studies may adopt DCM as well. The method we have used for obtaining EC has also been employed in several recent fMRI studies [10–14].

Brain regions (with exact region boundaries) involved in the affected network

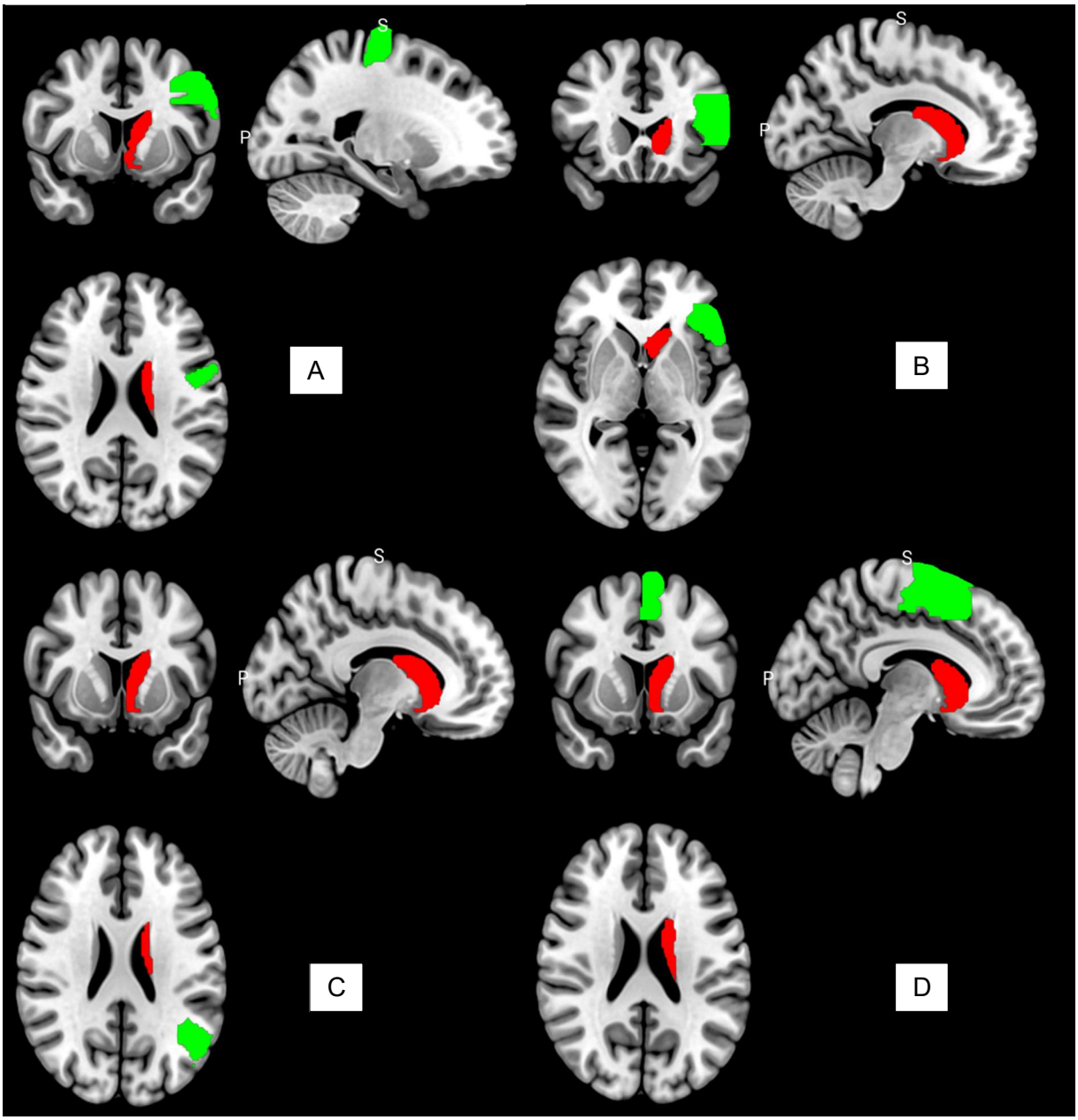

Figure S2: *Brain regions (with exact region boundaries) involved in the affected network. The regions were defined based on the WFU-pickatlas brain atlas. Red color indicates the left caudate, which is the source in all four connections. The Figure A to D show the connection of left caudate with left precentral gyrus (A), left frontal inferior triangular gyrus (B), left angular gyrus (C), and left supplementary motor area (D).*

Table S1 – Effect of condition on effective connectivity in patients with schizophrenia

			Areas & connectivity
SCZ	**BL**	**OXT**	Left caudate and left supplementary motor area ($p<0.008$) Left caudate and left precentral ($p < 0.009$) Left caudate and left frontal inferior triangular ($p<0.025$) Left caudate and left angular ($p<0.003$)
	BL	**PLA**	No significant finding
	PLA	**OXT**	Left caudate and left supplementary motor area ($p=0.027$) Left caudate and left precentral ($p =0.014$) Left caudate and left frontal inferior triangular ($p=0.015$) Left caudate and left angular ($p=0.069$)

Correlation with Behavior

As a previous study had reported relation between negative symptoms and response to oxytocin [15], we conducted a canonical correlation analysis (CCA) between connectivity variables on one-side and behavioral/symptom/demographic non-imaging measures on the other side [16]. The connectivity variables included the (i) change in connectivity between oxytocin and placebo in patients, and (ii) change in connectivity between oxytocin and baseline in patients, both for paths conforming to our hypotheses. The non-imaging measure included age (in years), years of education, SES (socio-economic status), Global Assessment of Functioning (GAF), Duration of illness, age of onset, PANSS (Positive and Negative Syndrome Scale) Positive, PANSS Negative, PANSS GP (General Psychopathology), PANSS Total, SANS (Scale for the Assessment of Positive Symptoms) Total, CGI (Clinical Global Impression) Severity, CDS (Calgary Depression Scale) Total, BCIS (Beck Cognitive Insight Scale) SR (self-reflectance), BCIS SC (self-certainty) and BCIS Composite. Permutation testing with 1000,000 iterations was used to find significant modes (latent variables that correlate with each other between the imaging and non-imaging measures) and their loadings [17].

Four modes were determined by the CCA algorithm. For the connectivity difference between oxytocin and placebo in patients, mode-3 was significant (FDR corrected p-values – mode-1=0.37, mode-2=0.29, mode-3=0.003 and mode-4=0.18). For the connectivity difference between oxytocin and placebo in patients, all three paths were positively correlated with SES and BCIS SR and negatively correlated with age of onset, PANSS Negative and CGI Severity. This shows that better the socioeconomic status and cognitive insight, earlier the age of onset and lesser the severity of symptoms, the greater the increase in connectivity with oxytocin as compared to placebo.

In Fig S3, we show the correlation of differences in behavioral scores with differences in connectivity values. It is noteworthy that there were no statistically significant differences between baseline and placebo scans as this was a criterion for the conjunction analysis. As this figure represents CCA models, please note that these differences themselves may not be statistically significant but can be significantly correlated with each other. It means that even small variations in connectivity between oxytocin and placebo mirrored corresponding small variations in demographic or clinical variables.

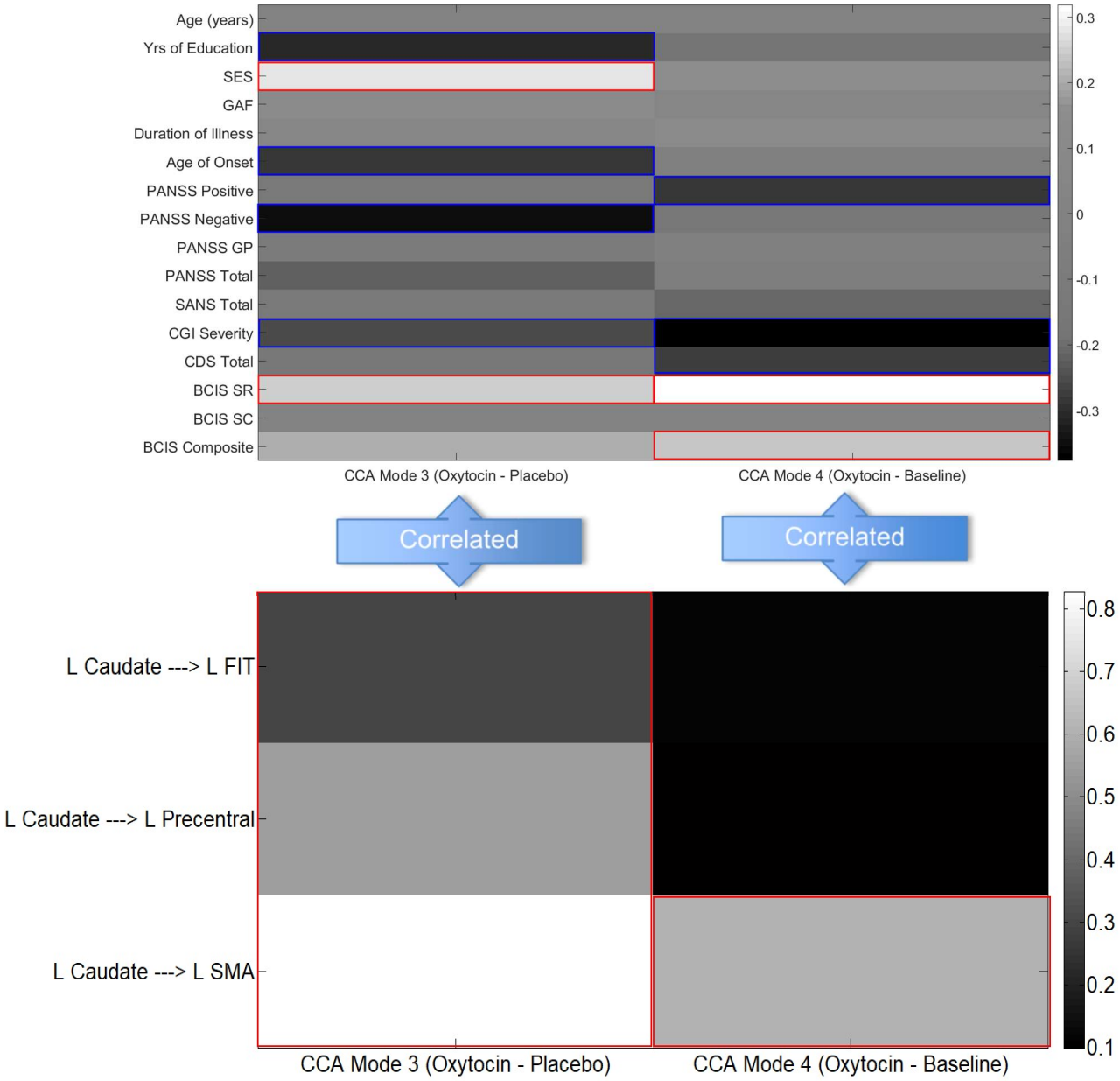

Figure S3: *The loadings of the CCA modes 3 and 4 on individual imaging and non-imaging measures. Significant loadings are shown in red (for positive correlations) and blue (for negative correlations). It is to be noted that for the connectivity difference between oxytocin and placebo/baseline in patients, mode 3/4 were significant, respectively*

References for the supplement section:

1. Roebroeck A, Formisano E, Goebel R. Mapping directed influence over the brain using Granger causality and fMRI. 2005;25:230–242.
2. Deshpande G, Libero LE, Sreenivasan KR, Deshpande HD, Kana RK. Identification of neural connectivity signatures of autism using machine learning. Frontiers in Human Neuroscience. 2013;7:1–15.
3. Deshpande G, Li Z, Santhanam P, Coles CD, Lynch ME. Recursive Cluster Elimination Based Support Vector Machine for Disease State Prediction Using Resting State Functional and Effective Brain Connectivity. 2010;5:1–10.
4. Ryali S, Supekar K, Chen T, Menon V. NeuroImage Multivariate dynamical systems models for estimating causal interactions in fMRI. NeuroImage. 2011;54:807–823.
5. Wen X, Rangarajan G, Ding M. Is Granger Causality a Viable Technique for Analyzing fMRI Data ? 2013;8.
6. David O, Guillemain I, Saillet S, Reyt S, Deransart C, Segebarth C, et al. Identifying Neural Drivers with Functional MRI : An Electrophysiological Validation. 2008;6.
7. Ryali S, Shih YI, Chen T, Kochalka J, Albaugh D, Fang Z, et al. Combining optogenetic stimulation and fMRI to validate a multivariate dynamical systems model for estimating causal brain interactions. NeuroImage. 2016. 2016. https://doi.org/10.1016/j.neuroimage.2016.02.067.
8. Katwal SB, Gore JC, Gatenby JC, Rogers BP. NeuroImage Measuring relative timings of brain activities using fMRI. NeuroImage. 2013;66:436–448.
9. Wang Y, David O, Hu X, Deshpande G. Can Patel's τ accurately estimate directionality of connections in brain networks from fMRI? Magnetic Resonance in Medicine. 2017;78:2003–2010.
10. Rangaprakash D, Dretsch MN, Yan W, Katz JS, Denney TS, Deshpande G. Hemodynamic variability in soldiers with trauma: Implications for functional MRI connectivity studies. NeuroImage Clinical. 2017;16:409–417.
11. Rangaprakash D, Deshpande G, Daniel TA, Goodman AM, Robinson JL, Salibi N, et al. Compromised hippocampus-striatum pathway as a potential imaging biomarker of mild-traumatic brain injury and posttraumatic stress disorder. Hum Brain Mapp. 2017;38:2843–2864.
12. Wheelock MD, Sreenivasan KR, Wood KH, ver Hoef LW, Deshpande G, Knight DC. Threat-related learning relies on distinct dorsal prefrontal cortex network connectivity. Neuroimage. 2014;102 Pt 2:904–912.
13. Grant MM, Wood K, Sreenivasan K, Wheelock M, White D, Thomas J, et al. Influence of early life stress on intra- and extra-amygdaloid causal connectivity. Neuropsychopharmacology: Official Publication of the American College of Neuropsychopharmacology. 2015;40:1782–1793.
14. Feng C, Deshpande G, Liu C, Gu R, Luo YJ, Krueger F. Diffusion of responsibility attenuates altruistic punishment: A functional magnetic resonance imaging effective connectivity study. Hum Brain Mapp. 2016;37:663–677.
15. Abram S v., de Coster L, Roach BJ, Mueller BA, van Erp TGM, Calhoun VD, et al. Oxytocin Enhances an Amygdala Circuit Associated with Negative Symptoms in Schizophrenia: A Single-Dose, Placebo-Controlled, Crossover, Randomized Control Trial. Schizophrenia Bulletin. 2020;46:661–669.

16. Wang HT, Smallwood J, Mourao-Miranda J, Xia CH, Satterthwaite TD, Bassett DS, et al. Finding the needle in a high-dimensional haystack: Canonical correlation analysis for neuroscientists. NeuroImage. 2020;216:116745.
17. Smith SM, Elliott LT, Alfaro-Almagro F, McCarthy P, Nichols TE, Douaud G, et al. Brain aging comprises manygeneticmodesand ofbiophysicalstructuralassociationsand functional change with distinct. ELife. 2020;9.